2009

On the stability of multibreathers in Klein-Gordon chains

V Koukouloyannis

PG Kevrekidis
University of Massachusetts - Amherst, kevrekid@math.umass.edu

On the stability of multibreathers in Klein-Gordon chains

Vassilis Koukouloyannis[1,2] **and Panayotis G Kevrekidis**[3]

[1] Department of Physics, Section of Astrophysics, Astronomy and Mechanics, Aristotle University of Thessaloniki, 54124 Thessaloniki, Greece

[2] Department of Civil Engineering, Technological Educational Institute of Serres, 62124 Serres, Greece

[3] Department of Mathematics and Statistics, University of Massachusetts, Amherst MA 01003-9305

E-mail: vkouk@physics.auth.gr

Abstract. In the present paper, a theorem, which determines the linear stability of multibreathers excited over adjacent coupled oscillators in Klein-Gordon chains, is proven. Specifically, it is shown that for soft nonlinearities, and positive nearest-neighbor inter-site coupling, only structures with adjacent sites excited out-of-phase may be stable, while only in-phase ones may be stable for negative coupling. The situation is reversed for hard nonlinearities. This method can be applied to n-site breathers, where n is any finite number and provides a detailed count of the number of real and imaginary characteristic exponents of the breather, based on its configuration. In addition, an $\mathcal{O}(\sqrt{\varepsilon})$ estimation of these exponents can be extracted through this procedure. To complement the analysis, we perform numerical simulations and establish that the results are in excellent agreement with the theoretical predictions, at least for small values of the coupling constant ε.

PACS numbers: 63.20.Pw, 05.45.Yv

AMS classification scheme numbers: 37K60, 37K45

1. Introduction

Intrinsic localized modes (ILMs or discrete breathers) have been a center of intense theoretical, numerical, as well as experimental investigations over the past two decades; see e.g. the reviews [1, 2, 3, 4]. Since their theoretical inception in the context of anharmonic nonlinear lattices [5, 6] and subsequent rigorous proof of existence, under appropriate nonresonance conditions [7], numerous experimental realizations of such structures have arisen in settings ranging from optical waveguides and photorefractive crystals, to micromechanical cantilever arrays and superconducting Josephson junctions, as well as Bose-Einstein condensates and electrical lattices, among many others [3].

While the most fundamental modes among these discrete breathers, namely the 1- and 2-site solutions have been analyzed in some detail, much less is known about the case of *multi-site breathers* or *multibreathers*. The latter were initially discussed in [7]. Since that pioneering work, a lot of effort has been invested in proving the existence of multibreathers in Klein-Gordon chains (e.g. [8, 9, 10]). Regarding the stability of these motions, in [11] some stability results are obtained using the formulation of [10], but these results are applicable only to few-site excitations. On the other hand, in [12] (see also the more recent discussion of [13]) some theorems about the stability of multibreathers are proven, using Aubry's band theory [4], which can be applied to an arbitrary number of site excitations.

In the present work, a n-site breather stability theorem is proven. It generalizes the two previously mentioned works, by proving a detailed counting result about the number of real and imaginary characteristic exponents of the corresponding breather for arbitrary configurations. It should be noted that this result proves a relevant statement made in [12] as a claim based in numerical findings. The relevant eigenvalues are estimated to $\mathcal{O}(\sqrt{\varepsilon})$. Our method is based on the notion of the effective Hamiltonian originally introduced in [14] and generalized in [15, 16]. This idea has already been used in order to prove existence and stability of multi-site breathers in hexagonal and honeycomb lattices [17, 18, 19]. Similar results have been acquired for the case of the discrete nonlinear Schrödinger (DNLS) lattice [20, 21, 22] and were recently used in the study of discrete solitons in hexagonal and honeycomb lattices in [23].

Our principal result shows that for soft nonlinearities and general, multi-site excitations, the relevant structures may only be stable (for positive values of the coupling) when the adjacent sites are out of phase by π with respect to each other. For negative values of the coupling, stability is possible for in-phase excitations. This situation is reversed in the case of hard nonlinearities (i.e., in-phase multibreathers are stable for positive weak coupling, while out-of-phase ones for negative, weak coupling).

Our presentation is organized as follows: in section 2 we define the system under consideration, in section 3 we set up the general conditions for existence of multibreather solutions, in section 4 we acquire the theorem about the stability of the previously mentioned solutions and finally in section 5 we perform some numerical calculations in order to verify our theoretical predictions.

2. Definition of the system - Terminology

We define our oscillators by an autonomous Hamiltonian of one degree of freedom

$$H_u = \frac{1}{2}p^2 + V(x)$$

where $V(x)$ is the potential function. In this case, the system is integrable since H_u is always an integral of motion. We assume that $V(x)$ possesses a minimum at $x = 0$ (without loss of generality) with $V''(0) = \omega_p^2$ with $\omega_p \in \mathbb{R}$.

Because of the time reversal symmetry $x(-t) = x(t), p(-t) = -p(t)$ the solution of the oscillator can be written as

$$x(t) = \sum_{n=0}^{\infty} A_n(J)\cos(nw) \tag{1}$$

where J, w are the action-angle variables. Note that in the action-angle variables the motion of the oscillator is described by

$$\begin{aligned} w(t) &= \omega t + w_0 \\ J(t) &= \text{const.} \end{aligned}$$

where ω is the frequency and w_0 is the initial phase of the periodic motion.

We construct our chain by considering a countable set of oscillators with a nearest-neighbor coupling through a coupling constant ε. The Hamiltonian then becomes

$$H = H_0 + \varepsilon H_1 = \sum_{i=-\infty}^{\infty}\left(\frac{1}{2}p_i^2 + V(x_i)\right) + \frac{\varepsilon}{2}\sum_{i=-\infty}^{\infty}(x_{i+1} - x_i)^2 \tag{2}$$

where x_i is the displacement from the equilibrium, and p_i the momentum of the i-th oscillator. Note that H_0 is trivially integrable, being separable.

3. Existence of multibreathers

Consider the "anticontinuous" limit $\varepsilon = 0$ where $n + 1$ adjacent "central" oscillators move in periodic orbits with frequency ω but arbitrary phases, while the the remaining "non-central" oscillators lie at rest $(x_i, p_i) = (0, 0)$. This state defines a trivially localized and time-periodic motion with period $T = 2\pi/\omega$. We seek conditions under which this motion can be continued for $\varepsilon \neq 0$ to provide a multibreather of the same frequency ω. In the next section we will determine the linear stability of the resulting solutions.

We apply the action-angle canonical transformation to the central oscillators. The system is described now by the set of variables (x_i, p_i, w_k, J_k) with $k \in \mathbb{S}$ and $i \in \mathbb{Z} \setminus \mathbb{S}$ where $\mathbb{S}$ is the set of "central" oscillators. So the periodic orbit which corresponds to the multibreather is described at time t by $z(t) = (x_i(t), p_i(t), w_k(t), I_k(t))$ with $z(t + T) = (x_i(t), p_i(t), w_k(t) + 2\pi, I_k(t))$.

In [14] (extended in [15] and [16]) it is proven that under the non-resonance condition $n\omega \neq \omega_p \forall n \in \mathbb{Z}$ there is an effective Hamiltonian H^{eff} whose critical points

correspond to periodic orbits (in fact, breathers) of the full system for ε small enough. The effective Hamiltonian is defined by

$$H^{\text{eff}}(I_i, A, \phi_i) = \frac{1}{T} \oint H \circ z(t)\ \mathrm{d}t,$$

where z is a periodic path in the phase space obtained by a continuation procedure for given relative phases ϕ_i, relative momenta I and symplectic "area" A. In the lowest order of approximation, the unperturbed orbit z_0 can be used instead of z. In our case, this coincides with the averaged Hamiltonian over an angle, for example $w_0 = \omega t + w_{0_0}$, due to the linear relationship of w_0 with t. Since, by construction, the resulting effective Hamiltonian does not depend on the selected angle w_0, and due to the nature of the system, a canonical transformation to the "central" oscillators is induced

$$\begin{array}{ll} \vartheta = w_0 & \mathcal{A} = J_0 + \ldots + J_n \\ \phi_1 = w_1 - w_0 & I_1 = J_1 + \ldots + J_n \\ \phi_2 = w_2 - w_1 & I_2 = J_2 + \ldots + J_n \\ \vdots & \vdots \\ \phi_n = w_n - w_{n-1} & I_n = J_n \end{array} \tag{3}$$

and, in the lowest order of approximation, the effective Hamiltonian becomes

$$H^{\text{eff}} = H_0(I_i) + \varepsilon \langle H_1 \rangle (\phi_i, I_i) \qquad i = 1 \ldots n \tag{4}$$

with

$$\langle H_1 \rangle = \frac{1}{T} \oint H_1 \mathrm{d}t$$

where the integration is performed along the unperturbed periodic orbit. Note that $\langle H_1 \rangle$ coincides with $\langle H_1 \rangle_{w_0}$, the average value of H_1 over the angle w_0 and since H^{eff} is independent of ϑ, A is a constant of motion.

As we have already mentioned, the critical points of this effective Hamiltonian correspond to breathers. But for non-degenerate critical points, to leading order in ε this condition reduces to the conditions (which were aquired also in [10])

$$\frac{\partial \langle H_1 \rangle}{\partial \phi_i} = 0, \quad \frac{\partial^2 \langle H_1 \rangle}{\partial \phi_i \partial \phi_j} \neq 0, \quad \left| \frac{\partial^2 H_0}{\partial J_i \partial J_j} \right| \neq 0 \Rightarrow \frac{\partial \omega_i}{\partial J_i} \neq 0, \quad \omega_p \neq k\omega. \tag{5}$$

Note that, since we consider central oscillators with the same frequency, condition (5c) can be reduced to $\frac{\partial \omega}{\partial J} \neq 0$. By taking into account (1) we get (see Appendix A for details)

$$\langle H_1 \rangle = -\frac{1}{2} \sum_{m=1}^{\infty} \sum_{i=1}^{n} A_m^2 \cos(m\phi_i) \tag{6}$$

hence, the condition (5a) becomes

$$\sum_{m=1}^{\infty} m A_m^2 \sin(m\phi_i) = 0 \tag{7}$$

which has at least the solutions

$$\phi_i = 0, \pi.$$

Intuitively, we expect that these are the only solutions, in this kind of systems, however, a general proof of this conjecture is not presently available [24].

It is interesting to note in passing here the similarity of the above conditions to the Lyapunov-Schmidt persistence conditions obtained in the context of the DNLS model in [20, 21, 22]. However, in the latter case, the presence of a single frequency enforces the $\phi_i = 0, \pi$ condition.

Remark 1. Although we don't have a full proof of the above assumption yet, physical considerations suggest its potential validity. For instance, consider the simplified setting wherein the displacement $x(w)$ (equivalently $x(t)$) from equilibrium is described by the truncated series $x(w) = A_0 + A_1\cos(w) + A_2\cos(2w)$. Then, the acceleration $a(w) \equiv \ddot{x}(w)$ reads $a(w) = -\omega^2\left[A_1\cos(w) + 4A_2\cos(2w)\right]$. Since we know that a in the two edges of the motion should be $a(0) < 0$ and $a(\pi) > 0$, this means that $A_1 + 4A_2 > 0$ and $A_1 - 4A_2 > 0$ and finally $A_1^2 > 16A_2^2$. Since for this case (7) reads $A_1^2\sin(\phi) + A_2^2\sin(2\phi) = \sin(\phi)[A_1^2 + 4A_2^2\cos(\phi)] = 0$, we conclude that in this special case, the above physical considerations preclude solutions other than $\phi = 0, \pi$.

4. Stability of the multibreather solutions

The linear stability of the fixed point of H^{eff} determines also the linear stability of the breather. This is proven in [14] for the first order approximation to H^{eff}, under the assumption of distinct eigenvalues of the first order matrix, and in [15] for the general case. This fact has already been used in order to study the stability of 3-site breathers in [18]. Again, there is a direct analog of this in the DNLS case, whereby the Jacobian of the Lyapunov-Schmidt conditions in [20, 21, 22] is, to leading order, directly analogous to the squared eigenvalues of the full linearization problem.

To make things more precise, the linear stability of a multibreather, is determined by its *Floquet multipliers* (see e.g. [4]), which are the eigenvalues of the monodromy matrix of the corresponding periodic orbit. If *all* the multipliers lie on the unit circle the breather is linearly stable, otherwise the breather is unstable. Due to the Hamiltonian character of the system if λ is a multiplier so are $\lambda^*, \lambda^{-1}, \lambda^{*-1}$. In particular, for multibreathers, when $\varepsilon = 0$ all the multipliers lie in two conjugate bundles at $e^{\pm i\omega_p T_b}$ except for $n+1$ pairs, which lie at unity and correspond to the central oscillators. When this solution is continued for $\varepsilon \neq 0$ the multipliers which belong to the two bundles, being of the same Krein kind (e.g. [25]), move along the unit circle to form the phonon band. On the other hand, one pair of the multipliers of the central oscillators will remain at 1 because of the corresponding invariance of the system while the rest can move either along the unit circle or outside the unit circle determining in this way the linear stability of the multibreather.

We define the *characteristic exponents* σ_i of the multibreather, or equivalently of the corresponding periodic orbit, as

$$\lambda_i = e^{\sigma_i T_b}.$$

The non-zero characteristic exponents of the central oscillators correspond to the eigenvalues of the $(2n \times 2n)$ *stability matrix* [14, 15] $\mathbf{E} = \mathbf{\Omega} D^2 H^{\text{eff}}$, where $\mathbf{\Omega} = \begin{pmatrix} \mathbf{O} & -\mathbf{I} \\ \mathbf{I} & \mathbf{O} \end{pmatrix}$ and $\mathbf{I}$ the $n \times n$ identity matrix. According to the above, for linear stability we demand that all the eigenvalues of $\mathbf{E}$ be purely imaginary. The stability matrix $\mathbf{E}$, to leading order of approximation and by taking into consideration (4), becomes

$$\mathbf{E} = \left(\begin{array}{c|c} \mathbf{A} & \mathbf{B} \\ \hline \mathbf{C} & \mathbf{D} \end{array}\right) = \left(\begin{array}{c|c} \varepsilon\mathbf{A_1} & \varepsilon\mathbf{B_1} \\ \hline \mathbf{C_0} + \varepsilon\mathbf{C_1} & \varepsilon\mathbf{D_1} \end{array}\right) = \left(\begin{array}{c|c} -\varepsilon\dfrac{\partial^2\langle H_1\rangle}{\partial\phi_i\partial I_j} & -\varepsilon\dfrac{\partial^2\langle H_1\rangle}{\partial\phi_i\partial\phi_j} \\ \hline \dfrac{\partial^2 H_0}{\partial I_i I_j} + \varepsilon\dfrac{\partial^2\langle H_1\rangle}{\partial I_i\partial I_j} & \varepsilon\dfrac{\partial^2\langle H_1\rangle}{\partial\phi_j\partial I_i} \end{array}\right). \tag{8}$$

Using (6), the elements of $\mathbf{E}$ take the form

$$\frac{\partial^2\langle H_1\rangle}{\partial\phi_i\partial I_j} = \sum_{m=1}^{\infty} mg(J)\sin(m\phi_i)$$

with $\quad g(J) = \dfrac{\partial}{\partial I_j}\left(A_m(J_{i-1})A_m(J_i)\right)|_{J_{i-1}=J_i=J} \quad$ and $\quad i,j = 1\ldots n,$

while, (Appendix B),

$$\frac{\partial^2 H_0}{\partial I_i\partial I_j} = \begin{cases} 2\dfrac{\partial\omega}{\partial J} & j = i \\ -\dfrac{\partial\omega}{\partial J} & j = i\pm 1 \\ 0 & \text{else} \end{cases} \qquad \textit{and} \qquad \frac{\partial^2\langle H_1\rangle}{\partial\phi_i\partial\phi_j} = \begin{cases} f(\phi_i) & j = i \\ 0 & j \neq i \end{cases}$$

where

$$f(\phi) = \frac{1}{2}\sum_{n=1}^{\infty} n^2 A_n^2 \cos(n\phi). \tag{9}$$

Since we consider solutions with $\phi_i = 0, \pi$, where $\mathbf{A} = \mathbf{D} = \mathbf{O}$, the stability matrix of (8) becomes

$$\mathbf{E} = \begin{pmatrix} \mathbf{O} & \mathbf{B} \\ \mathbf{C} & \mathbf{O} \end{pmatrix} = \begin{pmatrix} \mathbf{O} & \varepsilon\mathbf{B_1} \\ \mathbf{C_0} + \varepsilon\mathbf{C_1} & \mathbf{O} \end{pmatrix} \tag{10}$$

Due to Lemma 1, the $\frac{\partial^2\langle H_1\rangle}{\partial I_i\partial I_j}$ terms contribute only to higher (than the leading) order, and hence will not be considered further in what follows.

Lemma 1. *The leading order of approximation of the eigenvalues of* $\mathbf{E}$ *is* $\mathcal{O}(\sqrt{\varepsilon})$*. The term* $\mathbf{C_1} = \frac{\partial^2\langle H_1\rangle}{\partial I_i\partial I_j}$ *in (10) only affects the eigenvalues at* $\mathcal{O}(\varepsilon^{3/2})$*.*

The proof can be found in Appendix C. □

As it is also shown in Appendix C, up to the leading order of approximation, we have

$$\sigma_{\pm i} = \pm\sqrt{\varepsilon\,\chi_{1i}} + \mathcal{O}(\varepsilon^{3/2}) \quad i = 1\ldots n, \tag{11}$$

where $\sigma_{\pm i}$ (the characteristic exponents) are the eigenvalues of $\mathbf{E}$ and χ_{1i} are the eigenvalues of $\mathbf{B_1C_0}$. So, the sign of χ_{1i} define the stability of the multibreather. Let, $f_i = f(\phi_i)$. Then, $\mathbf{B_1C_0}$ becomes

$$\mathbf{B_1}\cdot\mathbf{C_0} = -\frac{\partial\omega}{\partial J}\mathbf{Z} = -\frac{\partial\omega}{\partial J}\begin{pmatrix} 2f_1 & -f_1 & 0 & & \\ -f_2 & 2f_2 & -f_2 & 0 & \\ & \ddots & \ddots & \ddots & \\ & 0 & -f_{n-1} & 2f_{n-1} & -f_{n-1} \\ & & 0 & -f_n & 2f_n \end{pmatrix} \tag{12}$$

Lemma 2. *Let z_i be the eigenvalues of $\mathbf{Z}$. Then, the number of positive z_i's equals the number of positive f_i's, while the number of negative z_i's equals the number of negative f_i's.*

The proof can be found in Appendix D. □

Lemma 3. *Assuming the absence of solutions of (5a) other than $\phi_i = 0, \pi$, then $f(0) > 0$ and $f(\pi) < 0$.*

Proof. The fact that $f(0) > 0$ is obvious from (9) since A_i are the Fourier coefficients of a smooth real function. On the other hand,

$$F(\phi) = -\frac{1}{2}\sum_{n=1}^{\infty} A_n^2\cos(n\phi)$$

is a continuous function. Since the values $\phi = 0, \pi$ correspond to the extrema of $F(\phi)$, because of continuity, one of them corresponds to a local minimum while the other corresponds to a local maximum. So, since $f(0) = \frac{\mathrm{d}^2F(\phi)}{\mathrm{d}\phi^2}\Big|_{\phi=0} > 0$ corresponds to the minimum, therefore $f(\phi) = \pi$ must correspond to the maximum of $F(\phi)$ and $f(\pi) = \frac{\mathrm{d}^2F(\phi)}{\mathrm{d}\phi^2}\Big|_{\phi=\pi} < 0$. □

Lemma 4. *If $\varepsilon\frac{\partial\omega}{\partial J} < 0$ and $\phi_i = \pi \quad \forall i = 1\ldots n$, or if $\varepsilon\frac{\partial\omega}{\partial J} > 0$ and $\phi_i = 0 \quad \forall i = 1\ldots n$, then all the eigenvalues of E are purely imaginary up to $\mathcal{O}(\sqrt{\varepsilon})$ terms.*

Proof. Due to (12), we have $\chi_{1i} = -\frac{\partial\omega}{\partial J}z_i$. So, by using (11) we get

$$\sigma_{\pm i} = \pm\sqrt{-\varepsilon\,\frac{\partial\omega}{\partial J}\,z_i} + \mathcal{O}(\varepsilon^{3/2}). \tag{13}$$

The sign of z_i is defined by the value of ϕ_i according to lemmas 2 and 3, which, in turn, completes the proof of the lemma. □

If the eigenvalues λ_i are imaginary and distinct up to $\mathcal{O}(\sqrt{\varepsilon})$ terms the higher order terms cannot push them outside the imaginary axis for a variance of ε, say $\Delta\varepsilon$, small enough, because of continuity. On the other hand, if the eigenvalues λ_i have multiplicity > 1 up to $\mathcal{O}(\sqrt{\varepsilon})$ terms the higher order terms can, in principle, push them outside the imaginary axis for $\Delta\varepsilon$ arbitrary small, which would cause complex instability, through a Hamiltonian Hopf bifurcation. This, however, cannot happen in our system since a specific symplectic signature property holds.

Lemma 5. *If the eigenvalues of* $\mathbf{E}$ *are imaginary up to* $\mathcal{O}(\sqrt{\varepsilon})$ *terms they remain imaginary up to all orders of approximation.*

Proof. If the eigenvalues of $\mathbf{E}$ are imaginary up to some order of approximation, then, according to [26], if the corresponding quadratic form of D^2H^{eff} is definite, then the eigenvalues remain imaginary for all orders of approximation. The matrix D^2H^{eff} is

$$D^2H^{\text{eff}} = \begin{pmatrix} \dfrac{\partial^2 H_0}{\partial J_i \partial J_j} & O \\ O & \dfrac{\partial^2 \langle H_1 \rangle}{\partial \phi_i \partial \phi_j} \end{pmatrix}$$

and the corresponding quadratic form is $\delta^2 H^{\text{eff}} = (\overline{I}, \overline{\phi}) \cdot D^2H^{\text{eff}} \cdot (\overline{I}, \overline{\phi})^T$, with $\overline{I} = (I_1, \ldots, I_n)$ and $\overline{\phi} = (\phi_1, \ldots, \phi_n)$. Finally we get

$$\delta^2 H^{\text{eff}} = \frac{\partial \omega}{\partial J}\left[I_1^2 + (I_2 - I_1)^2 + \ldots + (I_n - I_{n-1})^2 + I_n^2\right] + \varepsilon\left[f(\phi_1)\phi_1^2 + \ldots + f(\phi_n)\phi_n^2\right].$$

This quadratic form remains definite for all the configurations which are described in Lemma 4. So, even in the case of higher multiplicity, the imaginary eigenvalues of E remain on the imaginary axis. □

The sequence of the above lemmas leads to our main stability theorem, as follows:

Theorem 1. *Under the assumption that (7) has no other solutions than* $\phi_i = 0, \pi$*, then, if* $\varepsilon\frac{\partial \omega}{\partial J} < 0$ *the only configuration which leads to linearly stable multibreathers, for* $|\varepsilon|$ *small enough, is the one with* $\phi_i = \pi \quad \forall i = 1 \ldots n$ *(out-of-phase multibreather), while if* $\varepsilon\frac{\partial \omega}{\partial J} > 0$ *the only linearly stable configuration, for* $|\varepsilon|$ *small enough, is the one with* $\phi_i = 0 \quad \forall i = 1 \ldots n$ *(in-phase multibreather). Moreover, for* $\varepsilon\frac{\partial \omega}{\partial J} < 0$ *(respectively,* $\varepsilon\frac{\partial \omega}{\partial J} > 0$*), for unstable configurations, their number of unstable eigenvalues will be precisely equal to the number of nearest neighbors which are in (respectively, out of) phase between them.*

Proof. Since for a linear stable multibreather we need imaginary eigenvalues of E, the only possible configurations for stability are the ones described by the theorem, as it can be shown from lemmas 3 and 4. The multibreather will remain stable for small enough values of $|\varepsilon|$, until the eigenvalues which correspond to the central oscillators will collide with the linear spectrum, causing a Hamiltonian Hopf bifurcation, leading to complex instability. □

We note in passing that the above theorem bears a direct analogy to Theorem 3.6 of [20] for the DNLS case.

Remark 2. Note that if the the on-site potential is even $V(x) = V(-x)$ then the cosine Fourier series of $x(t)$ becomes

$$x(t) = A_0 + \sum_{n=1}^{\infty} A_{2n-1} \cos[(2n-1)w]$$

and $f(\phi)$ becomes

$$f(\phi) = \frac{1}{2} \sum_{n=1}^{\infty} (2n-1)^2 A_{2n-1}^2 \cos[(2n-1)\phi]$$

which means $f(\pi) = -\frac{1}{2} \sum_{n=1}^{\infty} (2n-1)^2 A_{2n-1}^2 < 0$. So, Theorem 1 can be reformulated without the need of exclusion of possible other solutions of (7).

5. Numerical Results

As a prototypical numerical demonstration, consider a chain consisting of oscillators with on-site quartic potential $V(x) = \frac{x^2}{2} - 0.27\frac{x^3}{3} - 0.03\frac{x^4}{4}$. This potential is softening $\left(\frac{\partial \omega}{\partial J} < 0\right)$ as it can be seen in figure 1. We will consider the orbit with period $T = \frac{2\pi}{\omega} = 7.434$ which corresponds to amplitude of oscillation $x_{max} = 1.949275 \Rightarrow J = 1.20306 \Rightarrow \frac{\partial \omega}{\partial J} = -0.224556$. For the same orbit we get $f(0) = 1.423404$ and $f(\pi) = -1.279544$.

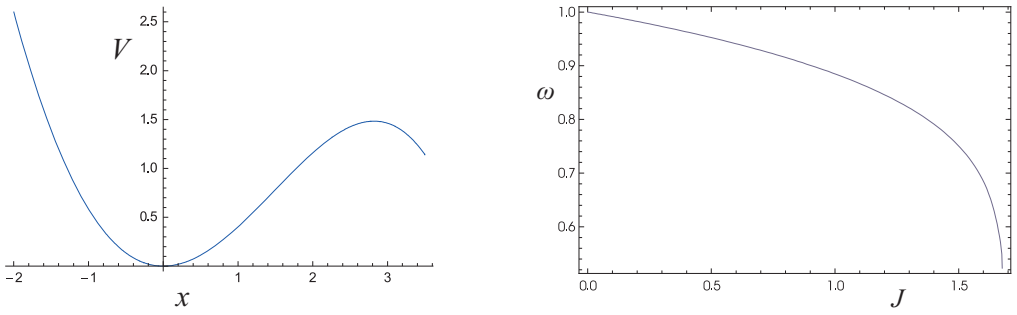

(a) (b)

Figure 1. Panel (b) shows the dependence of ω with respect to J for the specific $V(x)$ of panel (a).

5.1. 2-site multibreathers

We consider first the case of two cental oscillators (two oscillators moving at the anti-continuous limit). In this case there is only one $\phi = w_2 - w_1 = w_{20} - w_{10}$ and consequently only a pair of characteristic exponents. The leading order approximation of σ_i is, according to (13),

$$\sigma_{\pm 1} = \pm \sqrt{2\varepsilon \frac{\partial \omega}{\partial J} f(\phi)}. \tag{14}$$

The resulting 2-breathers are:

- The *in-phase* 2-breather with $\phi = 0$. In our example where $\varepsilon > 0$ and $\frac{\partial \omega}{\partial J} < 0$ we get $\sigma_{\pm 1} \in \mathbb{R}$, which leads to an *unstable* 2-breather. In figure 2a, the profile of the in-phase 2-breather is shown while in figure 2b the real part of the positive characteristic exponent of the central oscillator σ_1 as calculated by the numerical simulation is shown (solid line) together with the theoretical $\mathcal{O}(\sqrt{\varepsilon})$ prediction of σ_1 in (14) (dashed line). We can see that for small values of ε the agreement is excellent, while for larger values of ε, where the higher order terms of σ_1 become significant, the two lines start to diverge.
- The *out of phase* 2-breather with $\phi = \pi$ (see figure 3). In our example it is $\sigma_{\pm 1} \in \mathbb{I}$, which leads to a *linearly stable* 2-breather. In figure 3a, the profile of the out of phase 2-breather is shown, while in figure 2b the imaginary part of σ_1 is shown. The solid line represents the numerically calculated value while the dashed line is the theoretically approximated value. For small values of ε the two lines again nearly coincide, while for larger values of ε, the two lines diverge. For $\varepsilon \simeq 0.0254$ the solid line possesses a cusp which results from the collision of σ_1 with the linear spectrum. At this point two characteristic exponents (and their conjugates) acquire a nonzero real part, through a Hamiltonian Hopf bifurcation, and the corresponding multibreather becomes unstable. This is the typical mechanism through which multibreather solutions identified herein as stable for small ε eventually become unstable as the coupling is increased.

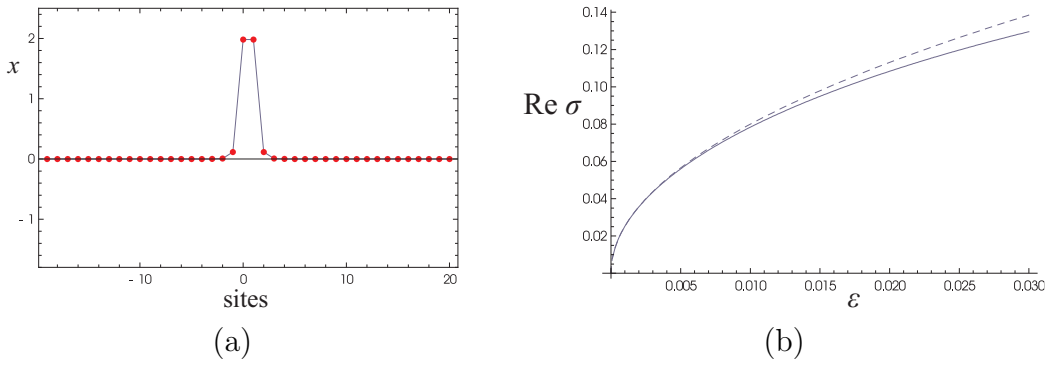

Figure 2. (a) The profile of an in-phase 2-site breather for $\varepsilon = 0.02$. In (b) the real part of σ_1, for increasing values of ε, is shown. The solid line represents the numerically calculated value, while the dashed one is the one resulting from (14).

5.2. 3-site multibreathers

The next step is to consider three central oscillators. In this case there exist two independent ϕ_i's, ϕ_1 and ϕ_2. So, there are three relevant configurations to examine, which correspond to the three possible combinations of ϕ_i.

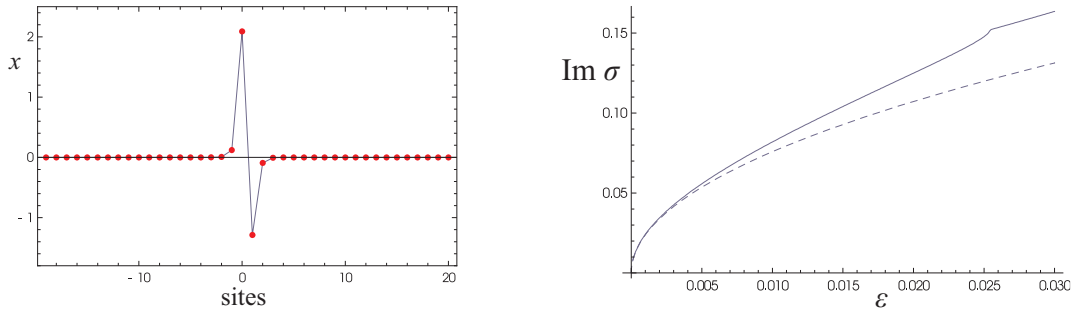

(a) (b)

Figure 3. (a) The profile of an out of phase 2-site breather for $\varepsilon = 0.02$. In (b) the imaginary part of σ_1, for increasing values of ε, is shown. The solid line represents the numerically calculated value, while the dashed one is the one resulting from (14).

- $\phi_1 = \phi_2 = 0$ *(In-phase multibreather).* Following (13), the leading order approximation of the four characteristic exponents of the 3-breather is

$$\sigma_{\pm 1} = \pm\sqrt{-\varepsilon \frac{\partial \omega}{\partial J} f(0)} \quad , \quad \sigma_{\pm 2} = \pm\sqrt{-3\varepsilon \frac{\partial \omega}{\partial J} f(0)}. \tag{15}$$

In our example this is an unstable configuration since $\sigma_{\pm 1,\pm 2} \in \mathbb{R}$. In figure 4a the profile of a 3-site in-phase breather for $\varepsilon = 0.02$ is shown, while in figure 4b the real part of the corresponding characteristic exponents $\sigma_{1,2}$ is shown. Again, the solid line denotes the numerically calculated values and the dashed ones represent the theoretical predictions. The agreement is very good, especially for small values of ε, illustrating the accuracy of our theoretical predictions.

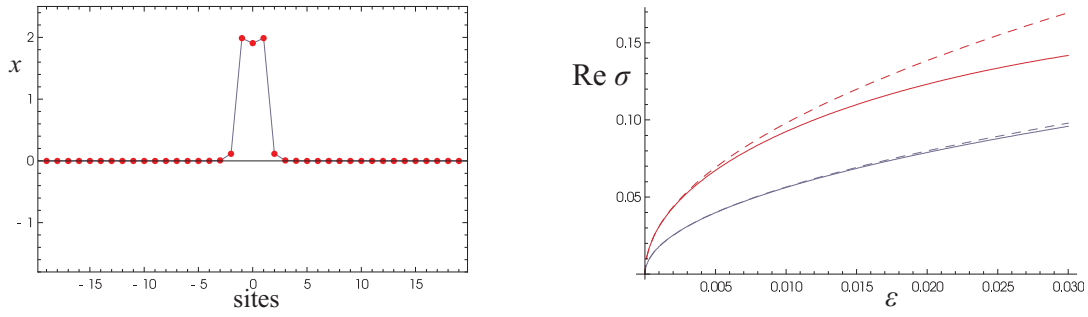

(a) (b)

Figure 4. (a) The profile of an in-phase 3-site breather for $\varepsilon = 0.02$. In (b) the real part of $\sigma_{1,2}$, for increasing values of ε, is shown. The solid lines represent the numerically calculated values, while the dashed lines correspond to the theoretical result of (15).

- $\phi_1 = \phi_2 = \pi$ *(Out-of-phase multibreather).* In this case, the leading order approximation of the corresponding characteristic exponents is

$$\sigma_{\pm 1} = \pm\sqrt{-\varepsilon \frac{\partial \omega}{\partial J} f(\pi)} \quad , \quad \sigma_{\pm 2} = \pm\sqrt{-3\varepsilon \frac{\partial \omega}{\partial J} f(\pi)}. \tag{16}$$

In our example this is a stable configuration since $\sigma_{\pm 1}, \sigma_{\pm 2} \in \mathbb{I}$. In figure 5a the profile of a 3-site out of phase breather is shown, while in figure 4b, the imaginary part of the corresponding characteristic exponents is shown. Once again, the agreement between the two lines can be noted, at least for small ε. For $\varepsilon \simeq 0.019$, the line which corresponds to σ_2 appears to change slope, a feature which is due to its collision with the multipliers stemming from the phonon band. For larger values of ε the multibreather is unstable.

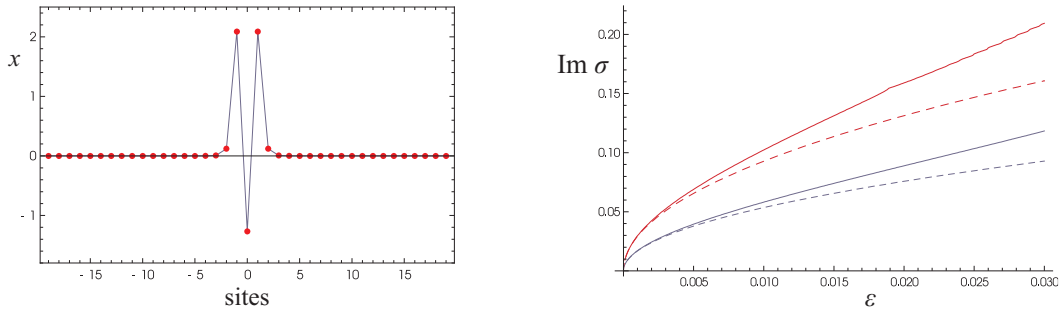

(a) (b)

Figure 5. (a) The profile of an out-of-phase 3-site breather for $\varepsilon = 0.02$. In (b) the imaginary part of $\sigma_{1,2}$, for increasing values of ε, is shown. The solid lines represent the numerically calculated values, while the dashed ones are the ones resulting from (16).

- $\phi_1 = 0, \phi_2 = \pi$. In this case, the corresponding leading order approximation of the characteristic exponents is

$$\begin{aligned} \sigma_{\pm 1} &= \pm \sqrt{-\varepsilon \frac{\partial \omega}{\partial J} \left(f_1 + f_2 - \sqrt{f_1^2 + f_2^2 - f_1 f_2} \right)} \\ \sigma_{\pm 2} &= \pm \sqrt{-\varepsilon \frac{\partial \omega}{\partial J} \left(f_1 + f_2 + \sqrt{f_1^2 + f_2^2 - f_1 f_2} \right)} \end{aligned} \tag{17}$$

with $f_1 = f(0)$ and $f_2 = f(\pi)$. In our example, $\sigma_{\pm 1} \in \mathbb{I}$ and $\sigma_{\pm 2} \in \mathbb{R}$ [it is straightforward to show that this will always be the case if $f_1 f_2 < 0$], so the corresponding configuration, shown in figure 6, is unstable. In figures 6(b) and 6(c), the imaginary and real parts of σ_1 and σ_2 are shown. Note that for $\varepsilon \simeq 0.03$, σ_1 enters the phonon band as can be seen in figure 6(c), where its real part becomes nonzero and the corresponding multibreather becomes unstable.

5.3. 5-site multibreathers

Our methodology can be numerically applied (through the simple numerical calculation of the eigenvalues of a $n \times n$ matrix), even when we cannot analytically calculate the eigenvalues of $\mathbf{E}$ ($\mathbf{Z}$). In this case we can still numerically calculate the eigenvalues of $\mathbf{Z}$ and get the $\mathcal{O}(\sqrt{\varepsilon})$ prediction from (13). In order to demonstrate this, we consider five central sites, so there exist four independent (relative angles) ϕ. A representative configuration is $\phi_1 = \phi_2 = 0$ and $\phi_3 = \phi_4 = \pi$ which results in an unstable multibreather

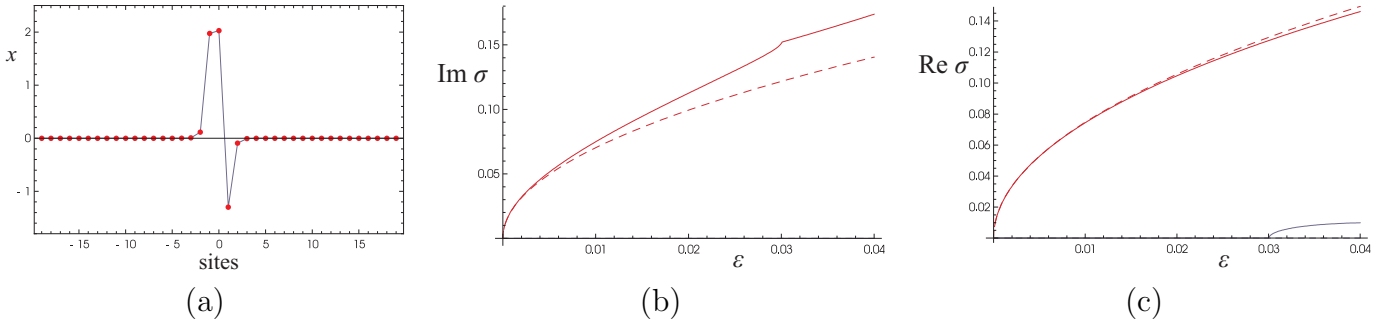

(a) (b) (c)

Figure 6. Panel (a) shows the profile of the multibreather corresponding to the $\phi_1 = 0, \phi_2 = \pi$ configuration for $\varepsilon = 0.02$. In (b) and (c) the imaginary and the real parts of $\sigma_{1,2}$, for increasing values of ε, are shown correspondingly. The solid lines represent the numerically calculated values, while the dashed ones are the ones resulting from (17).

with $\sigma_{1,2} \in \mathbb{R}$ and $\sigma_{3,4} \in \mathbb{I}$, as expected from our main theorem above (see e.g. figure 7).

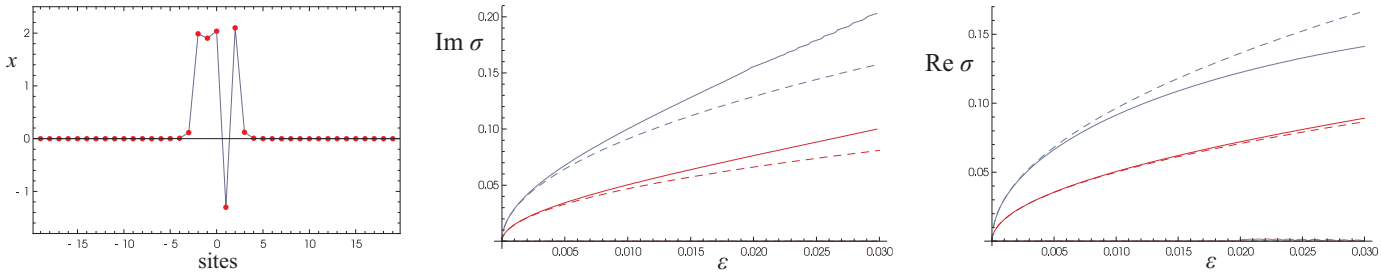

(a) (b) (c)

Figure 7. In (a) the profile of the 5-breather corresponding to the $\phi_{1,2} = 0, \phi_{3,4} = \pi$ configuration is shown for $\varepsilon = 0.02$. In (b) and (c) the imaginary and the real parts of σ_i, for increasing values of ε, are shown, respectively. The solid lines represent the numerically calculated values, while the dashed ones stem from the numerical calculation of the eigenvalues of the matrix $\mathbf{Z}$.

6. Conclusions

In the present paper, we proved a linear stability criterion for n-site multibreathers. This result generalizes the ones acquired in [11], which can determine the stability only for configurations up to three "central" oscillators, while it proves a counting result concerning the number of real and imaginary characteristic exponents of the breather, which is similar to the claim stated in [12]. In addition, our approach provides an $\mathcal{O}(\sqrt{\varepsilon})$ estimate of the characteristic exponents of the multibreather solution. Finally, the numerical simulations showed that our estimate is accurate for small values of ε, while it diverges for larger values of the coupling constant, which is naturally expected, since for this range of values the higher order terms of the expansion of the characteristic exponents become significant.

It would be especially interesting to extend these considerations to higher dimensional settings, to obtain a systematic characterization of vortex solutions and their stability, in square, as well as non-square geometries. Such efforts are currently in progress [17] and will be reported in future publications.

Appendix A. Calculation of $\langle H_1 \rangle$

The average value of H_1 is defined as

$$\langle H_1 \rangle = \frac{1}{T} \oint H_1 \mathrm{d}t,$$

where the integration is performed along the unperturbed periodic orbit. Since in the anti-continuous limit $\varepsilon = 0$ the only moving oscillators are the "central" ones, H_1 becomes

$$H_1 = \sum_{i=0}^{n} x_i^2 - \sum_{i=1}^{n} x_i x_{i-1}.$$

Therefore, only the mixed terms of H_1 interest us since, as we can easily conclude following the procedure below, the integration of the square terms over a period provides constant terms, i.e. terms independent of ϕ_i. We define $I_i = \int_0^T x_i x_{i-1} \mathrm{d}t$, so

$$\langle H_1 \rangle = -\frac{1}{T} \sum_{i=1}^{n} I_i + (\text{independent of } \phi_\mathrm{i} \text{ terms}). \tag{A.1}$$

Since at the anti-continuous limit the motion of the oscillators can be described by (1) we get, by dropping the constant term of the fourier series, for I_1

$$\begin{aligned} I_1 = \int_0^T x_1 x_0 \mathrm{d}t = \int_0^T \sum_{m=1}^{\infty} \sum_{s=1}^{\infty} A_m(J_1) \cos(m w_1) A_s(J_0) \cos(s w_0) \mathrm{d}t = \\ = \sum_{m=1}^{\infty} \sum_{s=1}^{\infty} A_m(J_1) A_s(J_0) \int_0^T \cos[m(\omega t + w_{10})] \cos[s(\omega t + w_{00})] \mathrm{d}t = \\ = \sum_{m=1}^{\infty} \sum_{s=1}^{\infty} \frac{A_m A_s}{2} \quad \left\{ \int_0^T \cos[(m+s)\omega t + (m w_{10} + s w_{00})] \mathrm{d}t \right. \\ \left. + \int_0^T \cos[(m-s)\omega t + (m w_{10} - s w_{00})] \mathrm{d}t \right\}. \end{aligned}$$

Without loss of generality, we can impose that $m, s > 0$. Then, the only terms that survive are the ones with $m = s$, so we get

$$I_1 = \sum_{m=1}^{\infty} \frac{A_m^2}{2} \int_0^T \cos[m(w_{10} - w_{00})] \mathrm{d}t = \sum_{m=1}^{\infty} \frac{A_m^2}{2} \int_0^T \cos[m(w_1 - w_0)] \mathrm{d}t = \sum_{m=1}^{\infty} \frac{T A_m^2}{2} \cos m\phi_1.$$

So, by (A.1) we get

$$\langle H_1 \rangle = -\frac{1}{2} \sum_{i=1}^{n} \sum_{m=1}^{\infty} A_m^2 \cos m\phi_i.$$

Appendix B. calculation of the $\frac{\partial H_0}{\partial I_i}$ terms

By taking the inverse transformation of (3) we get for the J_i's

$$\begin{aligned} J_0 &= A - I_1 \\ J_1 &= I_1 - I_2 \\ J_2 &= I_2 - I_3 \\ &\vdots \\ J_{n-1} &= I_{n-1} - I_n \\ J_n &= I_n \end{aligned} \tag{B.1}$$

Since the integrable part of the Hamiltonian is written by definition as $H_0 = H_0(J_0 \dots J_n)$ and consequently $H_0 = H_0(I_1 \dots I_n)$ we get by using (B.1)

$$\frac{\partial H_0}{\partial I_i} = \frac{\partial H_0}{\partial J_{i-1}}\frac{\partial J_{i-1}}{\partial I_i} + \frac{\partial H_0}{\partial J_i}\frac{\partial J_i}{\partial I_i} = -\frac{\partial H_0}{\partial J_{i-1}} + \frac{\partial H_0}{\partial J_i} = -\omega_{i-1}(J_{i-1}) + \omega_i(J_i),$$

where the last equality holds because H_0 is separable being the sum of one degree of freedom Hamiltonians. So, every frequency depends only on the corresponding action.

So, we have

$$\frac{\partial^2 H_0}{\partial I_i^2} = -\frac{\partial}{\partial I_i}\frac{\partial H_0}{\partial J_{i-1}} + \frac{\partial}{\partial I_i}\frac{\partial H_0}{\partial J_i} = -\frac{\partial^2 H_0}{\partial J_{i-1}^2}\frac{\partial J_{i-1}}{\partial I_i} + \frac{\partial^2 H_0}{\partial J_i^2}\frac{\partial J_i}{\partial I_i} = \frac{\partial^2 H_0}{\partial J_{i-1}^2} + \frac{\partial^2 H_0}{\partial J_i^2}$$

and for $\omega_i = \omega$ we get

$$\frac{\partial^2 H_0}{\partial I_i^2} = 2\frac{\partial \omega}{\partial J}.$$

Using the same arguments we get

$$\frac{\partial^2 H_0}{\partial I_{i+1}\partial I_i} = -\frac{\partial}{\partial I_{i+1}}\frac{\partial H_0}{\partial J_{i-1}} + \frac{\partial}{\partial I_{i+1}}\frac{\partial H_0}{\partial J_i} = \frac{\partial^2 H_0}{\partial J_i^2}\frac{\partial J_i}{\partial I_{i+1}} = -\frac{\partial^2 H_0}{\partial J_i^2}$$

which can be written as

$$\frac{\partial^2 H_0}{\partial I_{i+1}\partial I_i} = -\frac{\partial \omega}{\partial J}.$$

Appendix C. Expansion of the eigenvalues of E

Let

$$\mathbf{E} = \left(\begin{array}{c|c} \mathbf{O} & \mathbf{B} \\ \hline \mathbf{C} & \mathbf{O} \end{array}\right)$$

be the stability matrix, with eigenvalues σ_i. The eigenvalue problem for this matrix can be rewritten as

$$|\mathbf{BC} - \sigma^2 \mathbf{I}| = \mathbf{0}$$

or

$$|\mathbf{BC} - \chi\mathbf{I}| = \mathbf{0}. \tag{C.1}$$

Using the expansions $\chi_i = \chi_{0i} + \varepsilon\chi_{1i} + \varepsilon^2\chi_{2i}$, $\mathbf{B} = \varepsilon\mathbf{B_1}$ and $\mathbf{C} = \mathbf{C_0} + \varepsilon\mathbf{C_1}$, we get

$$|\varepsilon\mathbf{B_1C_0} + \varepsilon^2\mathbf{B_1C_1} - (\chi_0 + \varepsilon\chi_1 + \varepsilon^2\chi_2)\mathbf{I}| = 0.$$

Since this relation must hold in the limit $\varepsilon \to 0$, we get

$$|\chi_0\mathbf{I}| = 0 \Rightarrow \chi_{0i} = 0 \quad i = 1 \ldots n.$$

Hence, condition (C.1) becomes

$$|\varepsilon\mathbf{B_1C_0} + \varepsilon^2\mathbf{B_1C_1} - (\varepsilon\chi_1 + \varepsilon^2\chi_2)\mathbf{I}| = 0$$

or

$$|\varepsilon[\mathbf{B_1C_0} - \chi_1\mathbf{I} + \varepsilon(\mathbf{B_1C_1} - \chi_2\mathbf{I})]| = 0$$

or

$$\varepsilon^n\,|\mathbf{B_1C_0} - \chi_1\mathbf{I} + \varepsilon(\mathbf{B_1C_1} - \chi_2\mathbf{I})| = 0.$$

For $\varepsilon \neq 0$, this becomes

$$|\mathbf{B_1C_0} - \chi_1\mathbf{I} + \varepsilon(\mathbf{B_1C_1} - \omega\chi_2\mathbf{I})| = 0. \tag{C.2}$$

However, once again, this condition must hold for the $\varepsilon \to 0$ limit which reads

$$|\mathbf{B_1C_0} - \chi_1\mathbf{I}| = 0.$$

So, χ_{1i} depend only on $\mathbf{B_1}$ and $\mathbf{C_0}$, while $\mathbf{C_1}$ only affects the higher order terms. Since

$$\sigma^2 = \varepsilon\chi_1 + \varepsilon^2\chi_2$$

$$\sigma = \pm\sqrt{\varepsilon\chi_1}\sqrt{1 + \frac{\varepsilon\chi_2}{\chi_1} + \ldots}$$

$$\sigma = \pm\sqrt{\varepsilon\chi_1}(1 + \frac{\varepsilon\chi_2}{2\chi_1} + \ldots)$$

hence, up to terms $\mathcal{O}(\varepsilon)$, the eigenvalues of $\mathbf{E}$ are determined by $\mathbf{B_1}$ and $\mathbf{C_0}$, while the influence of $\mathbf{C_1}$ moves to terms of $\mathcal{O}(\varepsilon^{3/2})$.

Appendix D. Positive and negative eigenvalues of Z

For reasons of completeness, we also present a proof of the fact that the number of positive eigenvalues of $\mathbf{Z}$ (z_i) equals the number of positive f_is and the number of negative z_i equals the number of negative f_is. This can be done by induction, directly following the steps of Appendix C of [27].

First we define $\mathbf{Z}_n$ as

$$\mathbf{Z}_n = \begin{pmatrix} 2f_1 & -f_1 & 0 & & \\ -f_2 & 2f_2 & -f_2 & 0 & \\ & \ddots & \ddots & \ddots & \\ & 0 & -f_{n-1} & 2f_{n-1} & -f_{n-1} \\ & & 0 & -f_n & 2f_n \end{pmatrix}. \tag{D.1}$$

The determinant of $\mathbf{Z}_n$ is given [27] by

$$\det\mathbf{Z}_n = \det \begin{pmatrix} 2f_1 & 0 & & & \\ -f_2 & \frac{3}{2}f_2 & 0 & & \\ & \ddots & \ddots & \ddots & \\ & & -f_{n-1} & \frac{n}{n-1}f_{n-1} & 0 \\ & & & -f_n & \frac{n+1}{n}f_n \end{pmatrix} = (n+1)\prod_{i=1}^{n} f_i.$$

The claim holds for $\mathbf{Z}_i$ with $i = 1, 2, 3$. Let's assume that it holds for $\mathbf{Z}_{n-1}$. We will examine if it holds for $\mathbf{Z}_n$. Note that, we consider only the case $f_i \neq 0$, since in order to have $f_i = 0$, special symmetry conditions should hold.

Let's consider $f_i \neq 0$ for $i = 1 \dots n-1$. We define $\tilde{f} = (f_1 \dots f_{n-1})$ and $\widehat{f} = (\tilde{f}, \epsilon)$ with $\epsilon \in \mathbb{R}$, then the eigenvalues $z_1(\epsilon) \dots z_n(\epsilon)$ of $\mathbf{Z}_n$ are C^1 in ϵ; see e.g. [25].

Consider $\epsilon = 0$ first. Since $f_i \neq 0$ for $i = 1, \dots, n-1$ we have that $z_1(0), \dots, z_{n-1}(0) \neq 0$. In addition

$$\prod_{i=1}^{n-1} z_i(0) = n\prod_{i=1}^{n-1} f_i \neq 0 \Rightarrow \operatorname{sign}\left(\prod_{i=1}^{n-1} z_i(0)\right) = \operatorname{sign}\left(\prod_{i=1}^{n-1} f_i\right) \neq 0$$

and $z_n(0) = 0$ since the last row of $\mathbf{Z}_n$ vanishes. For $\epsilon \neq 0$ we have

$$\prod_{i=1}^{n} z_i(\epsilon) = (n+1)\epsilon\prod_{i=1}^{n-1} f_i$$

so, for small ϵ it is

$$\operatorname{sign}(z_n(\epsilon)) = \operatorname{sign}(\epsilon).$$

But,

$$\det\mathbf{Z}_n = (n+1)\epsilon\prod_{i=1}^{n-1} f_i \neq 0$$

is valid for every $\epsilon \neq 0$, so no eigenvalue can change sign as long as ϵ is nonzero. Consequently the claim holds for $\mathbf{Z}_n$ which coincides with $\mathbf{Z}$, so the lemma is proven.

Acknowledgments

The authors would like to thank Dmitry Pelinovsky for a critical read of the manuscript and numerous helpful remarks. PGK also gratefully acknowledges support from NSF-DMS-0349023, NSF-DMS-0806762 and the Alexander von Humboldt Foundation.

[1] S. Flach and C. R. Willis. Discrete breathers. *Physics Reports*, 295:181–264, 1998.

[2] R. S. MacKay. Discrete breathers: classical and quantum. *Physica A*, 288:174–198, 2000.

[3] S. Flach and A.V. Gorbach. Discrete breathers: Advances in theory and applications. *Physics Reports*, 267:1–116, 2008.

[4] S. Aubry. Breathers in nonlinear lattices: existence, linear stability and quantization. *Physica D*, 103:201–250, 1997.

[5] A.J. Sievers and S. Takeno. Intrinsic localized modes in anharmonic crystals. *Physical Review Letters*, 61:970–973, 1988.

[6] J.B. Page. Asymptotic solutions for localized vibrational modes in strongly anharmonic periodic systems. *Physical Review B*, 41:7835–7838, 1990.

[7] R. S. MacKay and S. Aubry. Proof of existence of breathers for time-reversible or Hamiltonian networks of weakly coupled oscillators. *Nonlinearity*, 7:1623–1643, 1994.

[8] T. Ahn. Multisite oscillations in networks of weakly coupled autonomous oscillators. *Nonlinearity*, 11:965–989, 1998.

[9] J. A. Sepulchre and R. S. MacKay. Localized oscillations in conservative or dissipative networks of weakly coupled autonomous oscillators. *Nonlinearity*, 10:679–713, 1997.

[10] V. Koukouloyannis and S. Ichtiaroglou. Existence of multibreathers in chains of coupled one-dimensional Hamiltonian oscillators. *Physical Review E*, 66:066602, 2002.

[11] V. Koukouloyannis and S. Ichtiaroglou. A stability criterion for multibreathers in klein-gordon chains. *International Journal of Bifurcation and Chaos*, 16:1823–1827, 2006.

[12] J. F. R. Archilla, J. Cuevas, B. Sanchez-Rey, and A. Alvarez. Demonstration of the stability or instability of multibreathers at low coupling. *Physica D*, 180:235–255, 2003.

[13] J. Cuevas, J. F. R. Archilla, and F. R. Romero. Effect of the introduction of impurities on the stability properties of multibreathers at low coupling. *Nonlinearity*, 18:769–790, 2005.

[14] T. Ahn, R. S. MacKay, and J-A. Sepulchre. Dynamics of relative phases: Generalised multibreathers. *Nonlinear Dynamics*, 25:157–182, 2001.

[15] R. S. MacKay. Slow manifolds. In T. Dauxois, A. Litvak-Hinenzon, R. S. MacKay, and A. Spanoudaki, editors, *Energy Localisation and Transfer*, pages 149–192. World Scientific, 2004.

[16] R. S. MacKay and J-A. Sepulchre. Effective Hamiltonian for travelling discrete breathers. *Journal of Physics A*, 35:3985–4002, 2002.

[17] V. Koukouloyannis, P. G. Kevrekidis, K. J. H. Law, I. Kourakis, and D. Frantzeskakis. Existence of discrete breathers in hexagonal and honeycomb lattices. (In preparation).

[18] V. Koukouloyannis and R. S. MacKay. Existence and stability of 3-site breathers in a triangular lattice. *J. Phys. A: Math. Gen.*, 38:1021–1030, 2005.

[19] V. Koukouloyannis and I. Kourakis. Multi-site localized modes in hexagonal dusty plasma lattices. (Submitted for publication in Phys. Rev. E).

[20] D. E. Pelinovsky, P. G. Kevrekidis, and D. J. Frantzeskakis. Stability of discrete solitons in nonlinear schrodinger lattices. *Physica D*, 212:1–19, 2005.

[21] D. E. Pelinovsky, P. G. Kevrekidis, and D. J. Frantzeskakis. Persistence and stability of discrete vortices in nonlinear schrödinger lattices. *Physica D*, 212:20–53, 2005.

[22] M. Lukas, D.E. Pelinovsky, and P.G. Kevrekidis. Lyapunov-schmidt reduction algorithm for three-dimensional discrete vortices. *Physica D*, 237:339–350, 2008.

[23] K. J. H. Law, P. G. Kevrekidis, V. Koukouloyannis, I. Kourakis, D. Frantzeskakis, and A. R. Bishop. Discrete solitons and vortices in hexagonal and honeycomb lattices: existence, stability and dynamics. *Physical Review E*, 78:066610, 2008.

[24] V. Koukouloyannis, P. G. Kevrekidis, and V. Rothos. Non-existence of phase-shift multibreathers

in 1D Klein-Gordon chains. (In preparation).

[25] V. A. Yacubovich and V. M. Starzhinskii. *Linear Differential Equations with Periodic Coefficients*. Wiley, New York, 1975.

[26] R. S. MacKay. Stability of equilibria of Hamiltonian systems. In R. S MacKay and J. D. Meiss, editors, *Hamiltonian Dynamical Systems*, pages 137–153. Adam Hilger, 1987.

[27] B. Sandstede. Stability of multiple-pulse solutions. *Transactions of the American Mathematical Society*, 350:429–472, 1998.